Eye (2022) 36:533–539
https://doi.org/10.1038/s41433-021-01461-w

The ROYAL COLLEGE of OPHTHALMOLOGISTS

ARTICLE

Peripapillary hyperreflective ovoid mass-like structures (PHOMS) in children

Ye Jin Ahn[1] · Yoo Yeon Park[1] · Sun Young Shin[1]

Received: 3 September 2019 / Revised: 21 January 2021 / Accepted: 9 February 2021 / Published online: 17 March 2021

Abstract

Background To analyse structural characteristics and perifoveal/peripapillary vasculature by OCT in children with peripapillary hyperreflective ovoid mass-like structures (PHOMS) and compare the results with those of normal subjects.

Methods Forty-five patients (84 eyes) under 18 years old with blurry disc margin were evaluated with spectral domain-OCT and swept course-OCT. Patients were divided into four groups, according to presence of PHOMS and then the size of the existing PHOMS. Eyes with visible optic disc drusen (ODD) were not included. Foveal avascular zone (FAZ) and vessel densities from macula and optic disc area were assessed and potential associations between vessel density and structural parameters, such as peripapillary retinal nerve fibre layer (pRNFL), and macular ganglion cell and inner plexiform layer (mGCIPL) thickness, were analysed.

Results Among 45 patients (eighty-four eyes), coexisting buried ODD were found only in eyes with PHOMS. The scleral canal diameter was significantly smaller in PHOMS positive eyes compared to control eyes. Vessel density measurements from the papillary, peripapillary and optic nerve head (ONH) regions in the large PHOMS group were significantly lower compared to the control group (papillary; $P = 0.014$, peripapillary; $P = 0.001$, ONH; $P = 0.046$). FAZ area and macular vessel densities showed no difference compared to normal eyes in all three PHOMS groups. pRNFL and mGCIPL thickness did not differ among four groups and correlations were also not significant.

Conclusions Children with PHOMS have smaller scleral canal and can entail buried ODD. Vessel densities of optic disc area in large PHOMS eyes are significantly lower than in normal eyes.

Introduction

Optic disc drusen (ODD) are calcified, hyaline, acellular deposits that are axoplasmic derivatives of disintegrated nerve fibres secondary to altered axoplasmic transport in an anatomically small scleral canal [1–3]. ODD are often discovered incidentally during ophthalmologic survey, because they are usually asymptomatic, and have a benign natural course [4]. Although the visual acuity is often not affected, visual field (VF) defects appear in up to 87% of all ODD cases [5], and reduction of the retinal nerve fibre layer (RNFL) may also be observed with optical coherence tomography (OCT) [6]. However, most of these functional and anatomical changes were found in cases of visible ODD, which is known to evolve from buried ODD, and so may not be detectable until the drusen become superficial [7]. Separating buried ODD from true papilledema, has been a long-time matter of interest, since the latter requires emergent neurologic workup and treatment. The introduction of enhanced depth imaging (EDI)-OCT and swept source (SS)-OCT has enabled visualisation of the optic nerve head (ONH) with higher resolution and investigation of the morphologic characteristics of the buried ODD [8, 9], but a number of studies have described buried ODD as peripapillary hyperreflective ovoid mass-like structures (PHOMS), which made the differential diagnosis even more confusing [10–13]. A recent guideline for diagnosing ODD using OCT by the Optic Disc Drusen Studies (ODDS) Consortium asserted that PHOMS are lateral bulging or herniation of

Supplementary information The online version contains supplementary material available at https://doi.org/10.1038/s41433-021-01461-w.

✉ Sun Young Shin
eyeshin@catholic.ac.kr

[1] Department of Ophthalmology and Visual Science, Seoul St. Mary's Hospital, College of Medicine, The Catholic University of Korea, Seoul, Republic of Korea

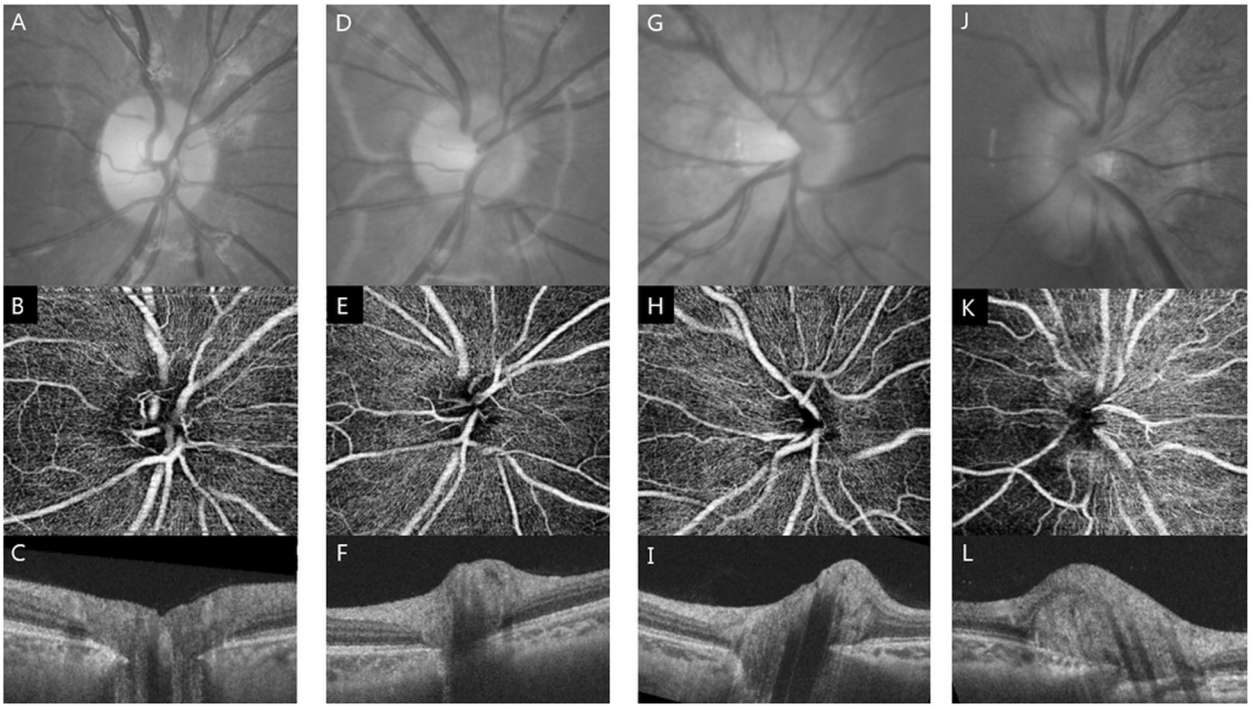

Fig. 1 Example results of a normal, small peripapillary hyperreflective ovoid mass-like structures (PHOMS), medium PHOMS and large PHOMS eyes, respectively. A, **B**, **C** Fundus photograph and swept-source OCTA images centred on the optic nerve head (ONH) of a normal individual. The OCTA image is brought from the ONH slab, which is analysed from the internal limiting membrane to 130 μm below the internal limiting membrane. **D**, **E**, **F** Corresponding images of a patient with small PHOMS. **G**, **H**, **I** Optic disc images of a patient with medium sized PHOMS. **J**, **K**, **L** Fundus photograph of a patient with large PHOMS shows obscured nasal disc margin, while the corresponding OCTA image shows a relatively low vessel density in the ONH region and the peripapillary region.

distended axons into the peripapillary retina, and should not be diagnosed as ODD [14].

Considering that in children, drusen are more likely to exist as a buried form, which can often be regarded as PHOMS, we investigated the structural and vascular characteristics of PHOMS found in children and its coexistence with ODD. Optical coherence tomography angiography (OCTA), which can be provided by SS-OCT, is a novel, non-invasive method of visualising the retinal microcirculation in a depth-resolved fashion, allowing segmentation and quantification of the retinal microvasculature [15]. We applied this new imaging modality to evaluate the foveal avascular zone (FAZ) and perifoveal/peripapillary vascular network density in children with varying sizes of PHOMS, and compared the findings to those in normal individuals.

Methods

Study population

This retrospective, observational case series was approved by the institutional review board of Seoul Saint Mary's Hospital and the study protocol followed the guidelines of the Declaration of Helsinki. Patients under 18 years of age with blurry disc margin who performed spectral domain (SD)-OCT and SS-OCT at Seoul St. Mary's Hospital from March 2018 to June 2018 were included in this study.

All patients underwent overall ophthalmic examination, including measurement of best-corrected visual acuity (BCVA), refractive error and axial length by way of the IOL master (IOL master 500, Carl Zeiss, Jena, Germany), as well as slit-lamp biomicroscopy and fundus photography. The mean peripapillary RNFL (pRNFL) thickness and the mean macular ganglion cell and inner plexiform layer (mGCIPL) thickness were obtained with SD-OCT (Cirrus HD-OCT, Carl Zeiss, Jena, Germany). In cases of suspicious optic disc oedema, neuro-ophthalmologic examinations including brain magnetic resonance imaging, VF test, and fluorescein angiography were performed for differential diagnosis. Patients with visible superficial drusen on fundus photography were not included in this study. Other exclusion criteria were clinically relevant media opacity preventing high-quality imaging, motion and blinking artifact, history of intraocular surgery, and the presence of any ocular or systemic diseases, especially those that could cause VF loss or optic disc abnormalities.

All patients were classified into four groups (Fig. 1). First, patients with normal SS-OCT findings were assigned

in the control group, and then the rest of the patients were sorted according to vertical height of PHOMS, which was previously applied as a qualitative estimate of the buried ODD size, as has been described elsewhere [12]; small (<300 μm), medium (300–500 μm) and large (≥500 μm). A peripapillary retinal thickness of ~300 μm was adopted as a cutoff value in determining small PHOMS. Patients with hyporeflective structures above the lamina cribrosa with a full or partial hyperreflective margin, most prominent superiorly, were considered to have coexisting ODD. The scleral canal diameter was measured by identifying the edge of Bruch's membrane on the opposing side of the optic disc, which was equivalent to the inner aspects of the scleral canal opening.

Image acquisition

The images were obtained using a swept-source OCTA device (DRI OCT Triton, Topcon Corporation, Tokyo, Japan) with a wavelength of 1050 nm, an acquisition speed of 100,000 A-scans per second and axial and transversal resolutions of 7 and 20 μm in tissue, respectively. OCT scans were taken from 4.5 × 4.5 mm cube centred on the fovea and ONH. En face images of the retinal vasculature in the macular area were generated from the superficial retinal capillary layer (SRL) and deep retinal capillary layer (DRL) by automated layer segmentation of the OCT instrument software. The SRL and DRL extended from the internal limiting membrane to the inner border of the inner nuclear layer and from the inner border of the inner nuclear layer to the outer border of the inner nuclear layer, respectively. On the other hand, the optic disc area was also automatically segmented into en face OCT slabs, and three slabs were selected for our study; (1) the papillary region was analysed from the internal limiting membrane to the outer border of the retinal pigment epithelium, (2) the peripapillary region, considered as the radial peripapillary capillary plexus was analysed from the internal limiting membrane to the outer border of the RNFL, and (3) the ONH region was analysed from the internal limiting membrane to 130 μm below the internal limiting membrane (Fig. 1).

Quantitative measurements

The GNU Image Manipulation Programme GIMP V.2.10 software (available in the public domain at http://gimp.org) was used to perform quantitative analysis. The FAZ area, defined by the area inside the inner border of the terminal capillary ring, was outlined manually for consideration of the SRL and DRL using the scissors tool of the GIMP software. The software calculated the outlined area in pixels, which was then converted to millimetres based on the scan dimensions (4.5 × 4.5 mm scan, 320 × 320 pixel resolution). The vessel density (VD) was evaluated using the colour selection tool of the GIMP software. For the macula cube scan, the mean brightness of the small vessels around the FAZ area was taken as a threshold, which was applied to binarize the SRL and DRL images. Any brightness value that was higher than the threshold was interpreted as vessels and VD was assessed as the ratio of area occupied by vessels. For the disc cube scan, the papillary region was defined as a 3.4 mm circular region centred on the ONH because in the 4.5 × 4.5 mm images, the majority of eyes were not centred on the optic disc. The VD of the peripapillary region was measured within a 700 μm wide annulus extending from the optic disc boundary. Finally, the inside disc area was measured for VD of the ONH region. The percentage area occupied by the large vessels and the microvasculature in the area of interest were calculated.

Statistical analysis

For statistical analysis, all data were analysed using SPSS Statistics 19.0 software (IBM Corporation, Armonk, NY, USA). The Shapiro–Wilk test was performed for normality. Descriptive statistics were calculated as the mean and standard deviation. The Kruskall–Wallis test was used for continuous data and the χ^2 test was used for categorical data. The comparison between each groups was performed by use of the Mann–Whitney U test. Correlations of the VD with OCT parameters were analysed by way of Pearson correlation test.

Results

A total of 84 eyes of 45 patients were included in the present study. PHOMS were discovered in 45 eyes (53.6%). The control group consisted of 39 eyes, 12 eyes in the small PHOMS group, 27 eyes in the medium PHOMS group and 6 eyes in the large PHOMS group. All of the participants were unrelated and no sibships were included. The mean ages of each group were 14.81 ± 2.12 years in the control group, 10.80 ± 4.21 years in the small PHOMS group, 11.80 ± 2.57 years in the medium PHOMS group, and 15.50 ± 6.36 years in the large PHOMS group, respectively, which showed no statistical significance ($P = 0.593$). The scleral canal diameter in eyes with PHOMS was smaller than in the control eyes ($P < 0.001$). No coexisting ODD was found in the control group, while 3 eye (25.0%) in the small PHOMS group, 10 eyes (37.0%) in the medium PHOMS group, and 3 eyes (50.0%) in the large PHOMS group showed underlying buried ODD ($P = 0.015$) (Fig. 2). There were no significant differences regarding gender, BCVA, refractive error and axial length among the groups (Table 1).

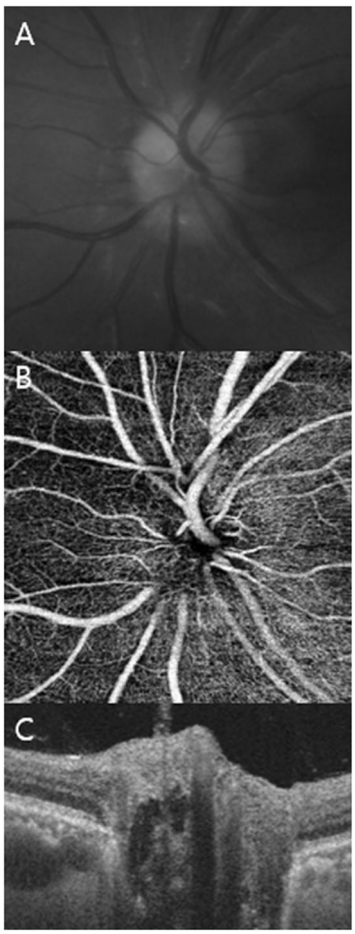

Fig. 2 PHOMS with optic disc drusen on SS-OCT. A Fundus photograph of the optic disc. **B** OCTA image from the optic nerve head slab. **C** Cross section of the optic disc, showing PHOMS and the underlying hyporeflective core with a partial hyperreflective margin.

Table 2 describes the OCTA and OCT parameters of the three PHOMS groups and the control group. Vasculature measurements from the macular cube scan, by FAZ area and vessel densities in the SRL and DRL, showed no statistical significance between PHOMS and control subjects, regardless of PHOMS size (all $P > 0.1$). On the other hand, the papillary, peripapillary and ONH vessel densities from the optic disc cube scan, also revealed no difference between the control group and the small PHOMS group and the medium PHOMS group, respectively. Conversely, the large PHOMS group showed significantly lower vessel densities in all three optic disc areas as compared with the control group (papillary: $P = 0.014$, peripapillary: $P = 0.001$, and ONH: $P = 0.046$, respectively). For the structural measurements, no significant differences were detected in all OCT parameters (pRNFL and mGCIPL thickness) among the control, and small, medium and large PHOMS groups. Furthermore, there were no meaningful correlations between the optic disc vessel densities and the pRNFL/mGCIPL thickness (Supplementary Table 1).

Discussion

The current study focused on PHOMS, which have been confused with buried drusen, especially in children. The scleral canal opening diameter was significantly smaller in eyes with PHOMS. Hyporeflective cores on OCT, indicating buried ODD, were only found in eyes with PHOMS, and none of the control eyes had buried ODD. There were no significant differences in RNFL and GCIPL thickness between PHOMS eyes with variable size and control eyes, suggesting neither of these OCT parameters were able to

Table 1 Clinical characteristics of patients with peripapillary hyperreflective ovoid mass-like structures (PHOMS).

	Small PHOMS ($n = 12$)	Medium PHOMS ($n = 27$)	Large PHOMS ($n = 6$)	Control ($n = 39$)	*P* value
Gender (male, *N*)	7	13	3	24	0.72†
Age (years)	10.80 ± 4.21	11.80 ± 2.57	15.50 ± 6.36	14.81 ± 2.12	0.60*
BCVA	0.90 ± 0.11	0.87 ± 0.14	0.91 ± 0.19	0.84 ± 0.19	0.87*
Refractive error (SE, D)	−1.11 ± 2.24	−1.36 ± 2.65	−2.34 ± 4.10	−1.48 ± 3.32	0.08*
Axial length (mm)	24.30 ± 0.86	24.40 ± 1.12	24.54 ± 2.02	23.91 ± 1.59	0.07*
PHOMS height (μm)	278.75 ± 22.27	398.20 ± 52.02	526.33 ± 285.04	–	<0.001*
Scleral canal diameter (μm)	1393 ± 868	1314 ± 702	1169 ± 525	1568 ± 757	<0.001*
Coexisting ODD (*N*, %)	3 (25.0)	10 (37.0)	3 (50.0)	0 (0)	0.015†

N number, *BCVA* best-corrected visual acuity, *SE* spherical equivalent, *D* dioptres, *ODD* optic disc drusen.

**P* value by Kruskall–Wallis test.

†*P* value by Chi-square test.

Table 2 Vasculature and structural measurements of patients in the macula and optic disc region.

	Small PHOMS ($n = 12$)	Medium PHOMS ($n = 27$)	Large PHOMS ($n = 6$)	Control ($n = 39$)	Small PHOMS vs. control	Medium PHOMS vs. control	Large PHOMS vs. control
OCTA parameters							
Macula images							
SRL FAZ (mm^2)	0.273 ± 0.08	0.324 ± 0.67	0.305 ± 0.15	0.367 ± 0.08	0.12	0.13	0.30
DRL FAZ (mm2)	0.440 ± 0.11	0.443 ± 0.10	0.497 ± 0.10	0.423 ± 0.98	0.43	0.36	0.75
SRL vessel density (ratio)	0.577 ± 0.06	0.593 ± 0.05	0.569 ± 0.04	0.587 ± 0.06	0.87	0.73	0.60
DRL vessel density (ratio)	0.703 ± 0.04	0.711 ± 0.04	0.684 ± 0.04	0.700 ± 0.05	0.58	0.14	0.97
Optic disc images							
Papillary vessel density (ratio)	0.823 ± 0.06	0.809 ± 0.05	0.799 ± 0.02	0.835 ± 0.01	0.75	0.26	0.014
Peripapillary vessel density (ratio)	0.856 ± 0.01	0.834 ± 0.05	0.812 ± 0.06	0.861 ± 0.02	0.76	0.10	0.001
ONH vessel density (ratio)	0.805 ± 0.08	0.796 ± 0.05	0.789 ± 0.06	0.800 ± 0.04	0.86	0.36	0.046
OCT parameters							
C/D ratio	0.40 ± 0.14	0.27 ± 0.13	0.27 ± 0.14	0.37 ± 0.16	0.22	0.06	0.25
pRNFL thickness (μm)	97.88 ± 15.03	99.27 ± 10.22	97.71 ± 16.33	98.02 ± 13.66	0.91	0.34	0.74
mGCIPL thickness (μm)	82.12 ± 5.57	83.00 ± 4.44	82.25 ± 4.03	83.10 ± 5.49	0.52	0.57	0.50

PHOMS peripapillary hyperreflective ovoid mass-like structures, *OCTA* optical coherence tomography angiography, *SRL* superficial retinal capillary layer, *DRL* deep retinal capillary layer, *FAZ* foveal avascular zone, *ONH* optic nerve head, *OCT* optical coherence tomography, *C/D* ratio cup disc ratio, *pRNFL* peripapillary retinal nerve fibre layer, *mGCIPL* macular ganglion cell and inner plexiform layer.

P value by Mann–Whitney *U* test.

discriminate PHOMS from normal ONH. In contrast, vessel densities measured from the papillary and peripapillary area in large PHOMS were significantly lower compared to normal eyes. However, the FAZ area and vessel densities from the SRL and DRL, indicating the microvascular supply in the macular area, showed no difference in large PHOMS eyes and control eyes. None of the vascular parameters in the small and medium PHOMS eyes were statistically distinguishable from the control eyes.

PHOMS have been mentioned in a number of reports, in association with ODD, that they might represent uncalcified precursors or variants of ODD [16, 17]. Traber et al. [17] examined 69 eyes of 38 patients and compared the morphologic characteristics of drusen in eyes with or without VF defects. They categorised patients by drusen morphology on EDI-OCT; (1) peripapillary subretinal hyperreflective drusen, which is currently referred as PHOMS, (2) granular hyperreflective drusen, and (3) confluent hyporeflective drusen. VF defects were more commonly found in larger ODD and/or confluent hyporeflective type ODD, whereas field defects were rare in patients with PHOMS, regarding field defects detected with PHOMS might have other underlying conditions. The authors claimed that the peripapillary hyperreflective ODD, granular ODD and confluent hyporeflective ODD are in extension of identical pathogenesis cascade.

In 2018, the ODDS Consortium reached a consensus for diagnosing ODD regarding its morphology, and defined ODD as hyporeflective structures with a full of partial hyperreflective margin [14]. In contrast, the authors recommend not to diagnose PHOMS as ODD, for the following reasons. First, PHOMS do not autofluoresce and are not visible on B-scan ultrasonography despite their superficial location, second, they do not correspond to clinically visible ODD, third, they are invariably located in the peripapillary circumference, and lastly, same OCT findings can be seen in patients with papilledema without ODD. Malmqvist et al. [18] demonstrated PHOMS in papilledema patients, such as idiopathic intracranial hypertension, anterior ischemic optic neuropathy, and central retinal vein occlusion. The axonal distension seen on EDI-OCT was remarkably similar to those of papilledema patients, and PHOMS disappeared without calcification when disc swelling resolved. Moreover, PHOMS were also observed in patients with myopic tilted discs, irrelevant to papilledema nor ODD. It is now suggested, PHOMS are nonspecific OCT findings of axonal distension and crowding that can be seen in acquired and dysplastic anomalies of the ONH.

Disturbance in the axonal metabolism in the presence of a small scleral canal is considered responsible for the ODD development [19]. This was supported by Lee et al. [16] who found a negative correlation between the height of ODD and the optic disc size. However, the mechanisms of prelaminar axonal distension and axoplasmic stasis is unclear, and the reason why some patients are predisposed to mitochondrial calcification, forming drusen and others are not. As Lee et al. [20] pointed out in a previous letter, if PHOMS were to be excluded from ODD, the discrimination of PHOMS from papilledema will need more caution, especially in children. We felt the necessity of investigating the morphologic characteristics of ONH in children, as the ODDS Consortium only studied patients older than 18 years. In the current study, the scleral canal diameter was significantly smaller in PHOMS positive children compared to normal children. Furthermore, underlying ODD was found only in the PHOMS group, while none of the control eyes showed a hyporeflective core in OCT. This result is consistent with previous studies, which reported PHOMS existing around the drusen in all cases of ODD [8, 12].

VF defects and RNFL thinning have been reported in patients with visible ODD [4, 6, 21, 22]. On the other hand, in cases of buried drusen, the average RNFL thickness was within normal range or even thicker than normal eyes and did not have VF defects [5]. Casado et al. [23] found that eyes with buried ODD presented abnormal thinning of average GCIPL than control eyes, suggesting GCIPL analysis might be an early structural indicator for neuronal loss. However, the mean age of patients with buried drusen was 31.8 ± 21.2 years, which was much higher compared to our study. Visible ODD is known to evolve from buried ODD [7]. Therefore, in children, drusen are more likely to be buried and may be more difficult to detect. In the present study, relatively young subjects were included, with a mean age of 13.23 ± 7.55 years. A previous study by Cennamo, reported decreased flow index and VD of ONH in ODD patients and thinner ganglion cell complex than normal controls, which significantly correlated with the OCTA parameters [24]. The discrepancy with our study might be attributed to the older age of participants, which was 22.05 ± 7.54 years in the previous study and the ODD type, which was not mentioned, and visible ODD might have been analysed as well. The results of our study suggest that in paediatric patients with large PHOMS, who are perhaps in the course of transition to visible ONHD or just a axoplasmic stasis, papillary/peripapillary VD decrease can be found on OCTA. It is unclear, whether the compression of neighbouring axons by PHOMS, or by the coexisting ODD caused the microvascular alterations in ONH. However, children with small scleral canal opening, are vulnerable to axoplasmic transport congestion, and therefore, more prone to develop PHOMS as well as ODD. Future studies are warranted to identify the relationship of PHOMS and ODD. In addition, long term evaluation is required since, abnormal OCTA findings might be an early indicator of functional alteration prior to RNFL or GCIPL change.

The limitations of our study are as follows. First, the overall sample size was small and inter-group variability exists, that the sample size of the large PHOMS group was much smaller than the other groups. Second, we were not able to measure retinal blood flow index, due to a software limitation of our OCT device. Third, VF test was not performed because it is difficult to perform, and is not routinely carried out among children. Lastly, our measurements were based on a single session. Further study dealing with longitudinal follow-up might provide better understanding on the mechanisms of PHOMS and its relationship with buried ODD.

To the best of our knowledge, this is the first study analysing structural characteristics and vessel densities in both macula and optic disc area in young patients with PHOMS. Children with PHOMS had smaller scleral canal diameter compared to normal children. Coexisting ODD were found only in the eyes with PHOMS. It seems that small and medium sized PHOMS, incidentally found in children do not cause vascular or structural alterations. However, large PHOMS, were associated with decreased peripapillary VD which might be an early indicator of functional deterioration before pRNFL and mGCIPL changes take place.

Summary

What was known before

- ODDS Consortium has recommended not to diagnose (PHOMS) as ODDs. However, until now, buried type ODDs are still confused with PHOMS.

What this study adds

- The characteristics of PHOMS found in children has not been studied previously. Herein, we introduce the structural features and vessel densities in macula and optic disc area in young patients with PHOMS.

Acknowledgements The authors thank all the patients for participating in this study.

Author contributions All authors contributed to the design and execution of this work, and all approved of this regarding submission.

Funding This study was supported by a National Research Foundation of Korea (NRF) grant funded by the Korea government (Ministry of Science and ICT, MSIT) (NRF-2019R1C1C1009503).

Compliance with ethical standards

Conflict of interest The authors declare no competing interests.

Publisher's note Springer Nature remains neutral with regard to jurisdictional claims in published maps and institutional affiliations.

References

1. Kamin DF, Hepler RS, Foos RY. Optic nerve drusen. Arch Ophthalmol. 1973;89:359–62.
2. Spencer WH. XXXIV Edward Jackson Memorial Lecture: drusen of the optic disc and aberrant axoplasmic transport. Ophthalmology. 1978;85:21–38.
3. Mullie MA, Sanders MD. Scleral canal size and optic nerve head drusen. Am J Ophthalmol. 1985;99:356–9.
4. Wilkins JM, Pomeranz HD. Visual manifestations of visible and buried optic disc drusen. J Neuroophthalmol. 2004;24:125–9.
5. Katz BJ, Pomeranz HD. Visual field defects and retinal nerve fiber layer defects in eyes with buried optic nerve drusen. Am J Ophthalmol. 2006;141:248–53.
6. Roh S, Noecker RJ, Schuman JS, Hedges TR 3rd, Weiter JJ, Mattox C. Effect of optic nerve head drusen on nerve fiber layer thickness. Ophthalmology. 1998;105:878–85.
7. Chang MY, Pineles SL. Optic disk drusen in children. Surv Ophthalmol. 2016;61:745–58.
8. Sato T, Mrejen S, Spaide RF. Multimodal imaging of optic disc drusen. Am J Ophthalmol. 2013;156:275–82.e1.
9. Silverman AL, Tatham AJ, Medeiros FA, Weinreb RN. Assessment of optic nerve head drusen using enhanced depth imaging and swept source optical coherence tomography. J Neuroophthalmol. 2014;34:198–205.
10. Lee KM, Hwang JM, Woo SJ. Optic disc drusen associated with optic nerve tumors. Optom Vis Sci. 2015;92:S67–75.
11. Bassi ST, Mohana KP. Optical coherence tomography in papilledema and pseudopapilledema with and without optic nerve head drusen. Indian J Ophthalmol. 2014;62:1146–51.
12. Lee KM, Woo SJ, Hwang JM. Morphologic characteristics of optic nerve head drusen on spectral-domain optical coherence tomography. Am J Ophthalmol. 2013;155:1139–47.e1.
13. Slotnick S, Sherman J. Disc drusen. Ophthalmology. 2012;119:652.
14. Malmqvist L, Bursztyn L, Costello F, Digre K, Fraser JA, Fraser C, et al. The optic disc drusen studies consortium recommendations for diagnosis of optic disc drusen using optical coherence tomography. J Neuroophthalmol. 2018;38:299–307.
15. Spaide RF, Klancnik JM Jr., Cooney MJ. Retinal vascular layers imaged by fluorescein angiography and optical coherence tomography angiography. JAMA Ophthalmol. 2015;133:45–50.
16. Lee KM, Woo SJ, Hwang JM. Differentiation of optic nerve head drusen and optic disc edema with spectral-domain optical coherence tomography. Ophthalmology. 2011;118:971–7.
17. Traber GL, Weber KP, Sabah M, Keane PA, Plant GT. Enhanced depth imaging optical coherence tomography of optic nerve head drusen: a comparison of cases with and without visual field loss. Ophthalmology. 2017;124:66–73.
18. Malmqvist L, Sibony PA, Fraser CL, Wegener M, Heegaard S, Skougaard M, et al. Peripapillary ovoid hyperreflectivity in optic disc edema and pseudopapilledema. Ophthalmology. 2018;125:1662–4.
19. Auw-Haedrich C, Staubach F, Witschel H. Optic disk drusen. Surv Ophthalmol. 2002;47:515–32.
20. Lee KM, Woo SJ, Hwang JM. Peripapillary hyperreflective ovoid mass-like structures: is it optic disc drusen or not? J Neuroophthalmol. 2018;38(4):567–8.
21. Savino PJ, Glaser JS, Rosenberg MA. A clinical analysis of pseudopapilledema. II. Visual field defects. Arch Ophthalmol. 1979;97:71–5.
22. Gili P, Flores-Rodriguez P, Martin-Rios MD, Carrasco Font C. Anatomical and functional impairment of the nerve fiber layer in patients with optic nerve head drusen. Graefe's Arch Clin Exp Ophthalmol. 2013;251:2421–8.
23. Casado A, Rebolleda G, Guerrero L, Leal M, Contreras I, Oblanca N, et al. Measurement of retinal nerve fiber layer and macular ganglion cell-inner plexiform layer with spectral-domain optical coherence tomography in patients with optic nerve head drusen. Graefe's Arch Clin Exp Ophthalmol. 2014;252:1653–60.
24. Cennamo G, Tebaldi S, Amoroso F, Arvanitis D, Breve M, Cennamo G. Optical coherence tomography angiography in optic nerve drusen. Ophthalmic Res. 2018;59:76–80.